J Hepatobiliary Pancreat Surg (2009) 16:816–823
DOI 10.1007/s00534-009-0124-4

ORIGINAL ARTICLE

Outcome of MR-guided percutaneous cryoablation for hepatocellular carcinoma

Tadashi Shimizu · Yusuke Sakuhara · Daisuke Abo · Yu Hasegawa · Yoshihisa Kodama · Hideho Endo · Hiroki Shirato · Kazuo Miyasaka

Received: 19 October 2008 / Accepted: 9 April 2009 / Published online: 23 May 2009

Abstract
Purpose To assess the mid-term results of MR-guided percutaneous cryoablation for small hepatocellular carcinoma (HCC).
Methods Using an argon-based cryoablation system, MR-guided percutaneous cryoablation was performed. The number of tumors was three or fewer. The maximum diameter of tumors was less than 5 cm when solitary and no more than 3 cm when multiple. The Kaplan–Meier method was used to calculate the survival of patients.
Results Among 15 patients, 16 tumors were treated. The maximum tumor diameter ranged from 1.2 to 4.5 cm, with a mean of 2.5 ± 0.8 cm (mean ± standard deviation). The volume of iceballs measured on MR-images was greater than that of the tumors in all cases. The follow-up period ranged from 10 to 52 months, with a mean of 36.6 ± 12.1 months. One-year and 3-year overall survival were 93.8 and 79.3%, respectively. The complete ablation rate was 80.8% at 3 years. Immediate complications were pneumothorax, hemothorax, and pleural effusion. An ablation zone was not absorbed and content exuded from a scar of the probe tract 4 months after cryoablation in one patient.
Conclusion MR-guided percutaneous cryoablation appears to be a feasible modality and potentially good option for the treatment of small HCC.

Keywords Hepatocellular carcinoma · Cryoablation · Magnetic resonance imaging

T. Shimizu (✉)
Department of Biomedical Science and Engineering, Faculty of Health Sciences, Hokkaido University, North-12 West-5, Kita-ku, Sapporo 060-0812, Japan
e-mail: tshim@hs.hokudai.ac.jp

Y. Sakuhara · D. Abo · Y. Hasegawa · H. Shirato
Department of Radiology, Hokkaido University Hospital, North-15 West-7, Kita-ku, Sapporo 060-8648, Japan

Y. Kodama
Department of Radiology, Teine Keijinkai Hospital, Maeda 1-12-1-40, Teine-ku, Sapporo 006-8555, Japan

H. Endo
Department of Radiology, Yokohama City Minato Red Cross Hospital, Shinyamashita 3-12-1, Naka-ku, Yokohama 231-8682, Japan

K. Miyasaka
Medical Image Lab., Inc., North-15 West-2, Kita-ku, Sapporo 001-0015, Japan

Introduction

Cryoablation is a type of thermal ablation, a category which also includes radiofrequency ablation (RFA), microwave coagulation therapy, and laser ablation. Cryoablation uses sub-zero temperatures to destroy tissue. The mechanisms of tissue injury are (1) intracellular crystallization, (2) osmotic dehydration of cells induced by freezing of extracellular water, and (3) thrombosis of small vessels [1]. It has been applied to primary and secondary hepatic malignancies intraoperatively, laparoscopically and percutaneously.

Onik et al. [2] showed the usefulness of ultrasonography (US) for monitoring frozen tissue in 1984. Thereafter, intraprocedural US monitoring was used mainly for cryoablation of liver tumors. It clearly depicts the near surface of the frozen tissue. However, because of acoustic shadows, the circumference of the iceball cannot be visualized. On the other hand, frozen areas in the tissue are clearly and precisely delineated on MR images [3]. Several years later, an MR-compatible cryoablation system was developed [4].

Cryoablation for metastatic liver tumors has been a frequent subject in the literature. On the other hand, reports on cryoablation for hepatocellular carcinoma (HCC) are less plentiful [5]. In particular, to our knowledge there are no reports of MR-guided and monitored cryoablation of HCC.

The purpose of this study was to describe the method of cryoablation of HCC and to evaluate its feasibility.

Materials and methods

The study protocol was approved by the ethics committee and written informed consent was obtained from all patients enrolled in this trial. Before a hepatic tumor was entered into the trial, it was necessary to diagnose it as HCC via a fine needle biopsy, tumor markers (AFP, PIV-KAII) or imaging. All patients were hospitalized during the procedure and for a few days to a week thereafter.

Eligibility

Patients were judged to be eligible to enter this trial after we confirmed that: (1) there was no extrahepatic tumor, (2) there were no more than 3 hepatic tumors, and (3) the maximum tumor diameter was less than 5 cm when solitary and less than 3 cm when in multiple. Computed tomography (CT) and magnetic resonance imaging (MRI) were used to select the patients.

Cryoablation system

We used a high-pressure argon-based cryoablation system (Cryo-Hit, Galil Medical Ltd., Yokneam, Israel) in which the cryoablation is based on the Joule–Thomson effect. When high-pressure (300 bars) argon gas expands to atmospheric pressure within the tip of the cryoprobe, it cools to an extremely low temperature, −185°C under ideal conditions. High-pressure helium gas at 38°C is used as a warming gas. The diameters of the cryoprobes were 2 and 3 mm for the 160-mm long probe, and 2 and 3 mm for the 210-mm long probe. The temperature was measured at the tip of the cryoprobe with a thermocouple and was displayed on the operation console monitor.

Procedures

The procedure has been widely documented in the literature [6]. The MR imager was a 0.3 T horizontal open-type MRI system (ARIS II, Hitachi Medical, Tokyo, Japan). Cryoablation was performed at −140°C. Two freeze-thaw cycles were used. The freezing time depended on the time required for iceball growth to appear on MR images. We employed passive thawing. To completely destroy the tumors, a 5 mm ablative margin on each side of the tumor was used whenever possible. Our study protocol permitted us a single session for each tumor.

Targeting and monitoring

Super-paramagnetic iron oxide was infused intravenously except in one patient who received intravenous infusion of gadolinium (Gd) contrast material. A sheath introducer (Medikit, Tokyo, Japan) to which an 18-gauge MR-compatible guiding needle (Daum Medical, Schwerin, Germany) was coaxially attached was placed with the aid of MR-fluoroscopic guidance under local anesthesia. After the guiding needle and dilator were withdrawn, the cryoprobe was introduced into the tumor through the sheath under MR-fluoroscopic guidance. We used three kinds of MR fluoroscopic sequences: T1-weighted (W) gradient echo (GrE) sequence (TR/TE/FA, 35/11.5/35; matrix,192 × 128; update 4 s); steady-state free-precession (SSFP) GrE echo planar (EPI) sequence (TR/TE/FA, 25/11.8/30; matrix, 100 × 228; update 2 s); time recovery steady-state free-precession (TR-SARGE) sequence (TR/TE/FA, 16/24.5/50; matrix, 152 × 128; update 2 s).

After the confirmation of the correct targeting of all the cryoprobes in the tumor, the iceball formation was viewed during the procedure using MR images to monitor how well the tumor and/or target was being covered by the iceball and whether or not any adjacent normal structures were affected at the same time. To confirm the cryoprobe positions and to monitor iceball formation, we used a multiplanar and multislice GrE sequence (TR/TE/FA, 120/10.5/60; update 15 s; 5 slices) and fast-spin echo sequence (TR/TE, 2500/75; update 15 s; 5 slices). The ablation was controlled on the basis of MR-image findings. The cryoprobes appeared clearly as very low-signal-intensity bands, and the iceballs appeared as sharply marginated regions of signal loss on intraprocedural MR images (Fig. 1).

Immediately after removal of the cryoprobes, gelatin sponge torpedoes were packed into the probe tracts and then the sheaths were withdrawn.

Assessment of treatment response

Contrast-enhanced MR images were taken 24 h, 2 weeks, and 6 weeks after the procedure. Blood and urine tests were performed on the same time schedule as the imaging. Contrast-enhanced MR or CT imaging and blood tests were performed regularly every 3 or 4 months after the procedure. We defined the 24-h ablation volume as the volume of lack of contrast-enhancement on Gd-contrast-enhanced MR images [4]. The volume of each tumor and 24-h ablation zone were estimated by measuring maximum

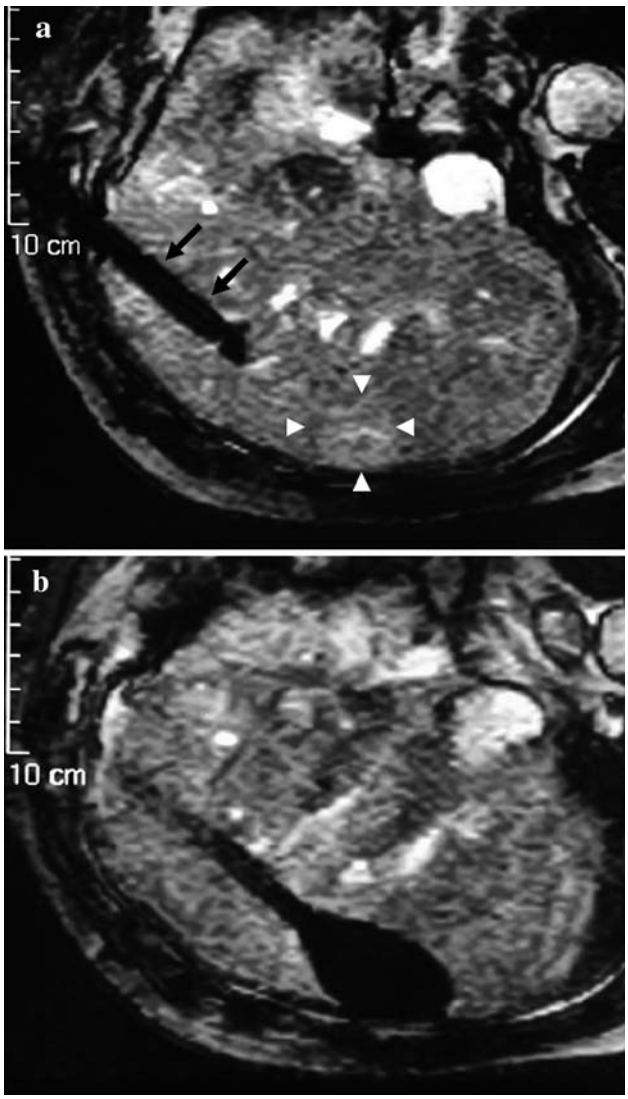

Fig. 1 A 69-year-old male with subcapsular HCC. **a** Intraprocedural transverse GrE sequence (TR/TE/FA, 120/10.5/60; update 15 s; 5 slices) shows cryoprobe (*solid arrow*) and tumor (*arrow head*). **b** Frozen area is clearly visible on MR image. Iceball formation is controlled within liver. We did not experience cracking or hemorrhaging

diameters in three planes and using the formula for the volume of an ellipsoid: (4/3) $\pi r_1 r_2 r_3$, where r_1, r_2, and r_3 are the maximum radii along three rectangular axes. Technical success was defined as a 24-h ablation volume that exceeded the tumor volume. The technical success rate was estimated by measuring the number of technical successes according to the protocol divided by the number of tumors originally entered into the study. Complete ablation was defined as benign peripheral enhancement on Gd-contrast-enhanced MR images 24 h after the procedure. The technique effectiveness rate was estimated by measuring the complete ablation divided by the number of tumors entered into the study.

Statistical analysis

The Kaplan–Meier method was used to calculate the survival of patients. In the assessment of the adverse reaction, common toxicity criteria of national cancer institute (CTC-NCI) version 2.0 was used for pain [7]. Other adverse reactions were reported descriptively.

Results

Fifteen patients were treated according to the protocol. Of these, 14 had one tumor each and one had two tumors; thus, 16 tumors were treated. The patients ranged in age from 45 to 72 years, with an average of 61.8 ± 9.0 (mean ± standard deviation) (Table 1). There were 14 patients with Child-Pugh class A hepatic dysfunction and one patient with class B. The maximum diameters of the tumors ranged from 1.2 to 4.5 cm, with the average at 2.5 ± 0.8 cm. The tumor volume ranged from 0.9 to 28.9 cm^3, with an average of 8.3 ± 7.7 cm^3. The follow-up period ranged from 10 to 52 months, with an average of 36.6 ± 12.5 months.

All patients were subjected to two freeze-thaw cycles and one to three cryoprobes, with an average of 2.1. The total freezing time ranged from 12 to 23 min, with an average of 14.5 ± 2.7 min.

The iceball volume ranged from 7.0 to 52.0 cm^3, with an average of 24.3 ± 13.9 cm^3. In all cases, the iceball volume measured on intraprocedural MR images exceeded the tumor volume (Table 2). Fourteen tumors were treated according to the protocol, and thus the technical success rate was 87.5% (14/16); in one patient, the 24-h ablation volume was less than that of the tumor. The technique effectiveness rate was evaluated to be 93.8% (15/16); irregular peripheral enhancement was seen in one patient and judged not to have been treated effectively (Fig. 2). The 24-h ablation volume ranged from 5.4 to 68.1 cm^3, with an average of 29.7 ± 17.3 cm^3. The average 24-h ablation volume was slightly larger than the iceball volume. The 24-h ablation volume was at least 10% larger than iceball volume in 11 of the 16 tumors. The mean iceball volume was not significantly different from the mean 24-h ablation volume ($p = 0.10$) (Table 3).

One-year and 3-year overall survival were 93.8 and 79.3%, respectively (Fig. 3a). Three patients died at 10, 27, and 30 months after cryoablation. The cause of death in each of these cases was tumor progression.

The complete ablation rate was 80.8% at 3 years (Fig. 3b). Local progression occurred in 3 patients at 4, 4.5, and 22 months. Of the 3 local progressions, 2 were from patients who had received incomplete ablation. Among the

Table 1 MR-guided percutaneous cryoablation of liver tumors: patient population, tumor characteristics, and ablation parameters

Patient no.	Tumor no.	Cryoablation no.	Age	Sex	Location (Couinaud segment)	Maximum tumor diameter (cm)	First freezing time (min)	Thawing time (min)	Second freezing time (min)	Total freezing time (min)
1	1	1	61	M	S8	2.0	5	2	8	13
2	2	2	59	M	S6	1.2	5	3	7	12
3	3	3	46	M	S5	2.8	7	2	6	13
4	4	4	65	F	S8	4.5	7	2	5	12
5	5	5	60	F	S8	2.3	7	2	7	14
6	6	6	56	M	S5/6	1.8	7	2	7	14
	7	15			S8	1.8	8	2	7	15
7	8	7	72	M	S5	3.2	7	2	8	15
8	9	8	72	F	S2	3.5	8	2	5.5	13.5
9	10	9	72	F	S7	2.2	8	3	5	13
10	11	10	69	M	S8	2.6	7	2	5	12
11	12	11	45	M	S8	2.5	8	2	7	15
12	13	12	72	M	S5	3.5	8	2	10	18
13	14	13	65	M	S8	1.8	11	2	12	23
14	15	14	58	F	S7	2.8	8	2	7	15
15	16	16	55	F	S6/7	2.0	8	2	7	15

Table 2 Comparison of tumor sizes versus maximum iceball sizes measured on intraprocedural MR images and the number and diameter of cryoprobes

Cryoablation no.	Number of cryoprobes used	Diameter of cryoprobes (mm)	Tumor maximum diameter (cm × cm × cm)	Tumor volume (cm^3)	Maximum iceball size (cm)	Iceball volume (cm^3)
1	2	2	2.0 × 1.6 × 1.7	2.8	2.3 × 3.0 × 4.2	15.2
2	2	2	1.2 × 1.2 × 1.2	0.9	4.0 × 2.0 × 2.0	8.4
3	3	2	2.8 × 2.5 × 2.0	7.3	5.0 × 3.0 × 2.7	21.2
4	3	3	4.5 × 3.5 × 3.5	28.9	4.8 × 3.8 × 3.8	36.3
5	1	3	2.3 × 2.3 × 2.3	6.4	4.8 × 2.8 × 2.8	19.7
6	2	3	1.8 × 1.5 × 1.5	2.1	3.7 × 1.8 × 2.0	7.0
7	3	3	2.8 × 2.9 × 3.2	13.6	3.5 × 6.3 × 4.5	52.0
8	3	3	3.4 × 3.1 × 3.5	19.3	4.1 × 5.6 × 4.3	51.7
9	2	3	2.1 × 2.2 × 2.0	4.8	2.3 × 3.5 × 3.2	13.5
10	1	3	2.6 × 2.2 × 2.4	7.2	4.2 × 3.0 × 3.0	19.8
11	2	3	2.0 × 2.5 × 2.0	5.2	2.8 × 4.8 × 3.5	24.6
12	3	3	3.5 × 3.0 × 3.0	16.5	4.0 × 4.2 × 3.9	34.3
13	1	3	1.5 × 1.8 × 1.8	2.5	2.0 × 4.0 × 2.5	10.5
14	2	3	2.8 × 2.7 × 2.5	9.9	3.4 × 3.5 × 3.1	19.3
15	2	3	1.8 × 1.5 × 1.5	2.1	3.4 × 4.0 × 3.0	21.4
16	2	3	2.0 × 1.7 × 1.8	3.2	3.5 × 4.4 × 4.2	33.9

Tumor size represents the largest diameter measured in all three dimensions on preprocedural MR images; iceball size represents the largest two short-axis diameters and the long-axis diameter of the largest iceball measured on intraprocedural MR images. Volumes were calculated using the formula for the volume of an ellipsoid

15 lesions which had received complete ablation, local progression was observed in one lesion.

New foci appeared in another segment in 8 patients during the follow-up period. We chose other modalities for these foci because our protocol permitted only one session for each tumor and limited the period of treatment with cryoablation. Additional treatments were trans-catheter arterial chemo-embolization (TACE) in 3 patients and RFA

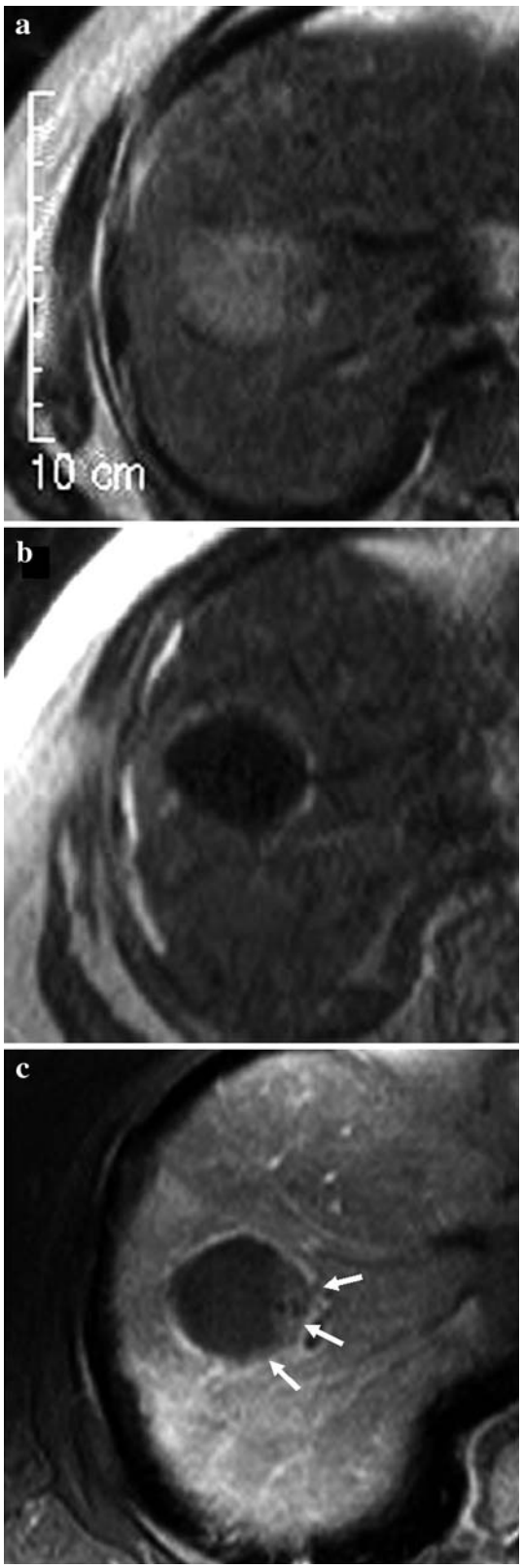

Fig. 2 A 65-year-old female with HCC in segment 8. **a** Preprocedural SPIO-enhanced T2 W MR image (TR/TE; 2000/100, matrix size 224 × 128, slice thickness 10 mm) shows tumor as high-intensity area (4.5 × 3.5 × 3.5 cm) in segment 8. **b** Although iceball is clearly visible on T2-weighted MR image (TR/TE; 2300/100, matrix size 224 × 128, slice thickness 8 mm), it is uncertain whether ablative margin is appropriate or not. **c** Gd-enhanced dynamic MR image (TR/TE; 288/4.75, matrix size 320 × 192, slice thickness 8 mm) reveals irregular peripheral enhancement (*arrow*) in medial side of the ablation zone 1 day after procedure

in 3 other patients. One patient who had received TACE died of HCC at 10 months after initial treatment. One patient who had received TACE was alive with tumor at the last follow-up, at 32 months after initial treatment. Four other patients were alive, without evidence of a tumor, with a median follow-up between 38 and 52 months after the initial treatment. No patients experienced distant metastasis or dissemination.

During the procedure, moderate pain was experienced by one patient. Nine patients complained of NCI-CTC version 2.0 grade 1 pain at the puncture site after the procedure for 1–10 days, and the average was 3.3 ± 2.8 days. One patient had grade 2 pain for 2 days.

No patients complained of pain during freeze-thaw cycles. Immediate complications (6–24 h following the procedure) were pneumothorax in 1, hemothorax in 1, and pleural effusion in 2. All these complications healed with conservative management. Post ablation syndrome, which is a transient self-limiting symptom or a sign complex of low-grade fever and general malaise, was observed in 10 patients. These symptoms persisted for 1–10 days.

Each patient experienced at least one of three periprocedural complications: mild, transient increases in serum aspartate aminotransferase (AST), alanine aminotransferase (ALT), and lactic acid dehydrogenase (LDH). The serum myoglobin level was increased in 2 patients. Transient increases in serum blood urea nitrogen (BUN) and creatinine levels were observed in 3 patients. Platelet counts decreased slightly and recovered to preprocedural levels in all patients. The preprocedural platelet count ranged from 6.2×10^4/ml to 21.6×10^4/ml, with an average of $12.9 \pm 4.7 \times 10^4$/ml. The minimum periprocedural platelet count ranged from 4.0×10^4/ml to 16.1×10^4/ml, with an average of $10.3 \pm 4.0 \times 10^4$/ml.

A delayed complication was observed in one patient: an ablation zone was not absorbed on follow up CT and MR images and a content of the ablation zone exuded from a scar of the probe tract 4 months after cryoablation, without pain or fever in one patient. A drainage tube was placed immediately, a small amount of necrotic material was drained, and the tube was withdrawn after 4 days. Histopathological examination revealed neither viable tumor cells nor bacteria were in the content. Eight months later, the ablated region had been spontaneously absorbed and a scar remained on CT images.

Table 3 Comparison of intraprocedural iceball volume with 24-h ablated volume

Cryoablation no.	Iceball maximum diameter (cm × cm × cm)	Iceball volume (cm^3)*	24-h ablated volume maximum diameter (cm × cm × cm)	24-h ablated volume (cm^3)*
1	2.3 × 3.0 × 4.2	15.2	2.8 × 2.5 × 4.6	16.9
2	4.0 × 2.0 × 2.0	8.4	3.8 × 1.6 × 1.7	5.4
3	5.0 × 3.0 × 2.7	21.2	4.8 × 3.0 × 3.2	24.1
4	4.8 × 3.8 × 3.8	36.3	3.6 × 4.2 × 4.2	33.3
5	4.8 × 2.8 × 2.8	19.7	6.2 × 3.2 × 5.0	51.9
6	3.7 × 1.8 × 2.0	7.0	4.5 × 1.8 × 3.0	12.7
7	3.5 × 6.3 × 4.5	52.0	6.1 × 3.2 × 4.0	40.9
8	4.1 × 5.6 × 4.3	51.7	6.5 × 5.0 × 4.0	68.1
9	2.3 × 3.5 × 3.2	13.5	2.1 × 3.0 × 3.0	9.9
10	4.2 × 3.0 × 3.0	19.8	4.5 × 2.9 × 4.0	27.3
11	2.8 × 4.8 × 3.5	24.6	4.8 × 3.1 × 4.0	31.2
12	4.0 × 4.2 × 3.9	34.3	4.2 × 2.2 × 3.2	15.5
13	2.0 × 4.0 × 2.5	10.5	4.6 × 2.1 × 3.0	15.2
14	3.4 × 3.5 × 3.1	19.3	6.1 × 3.3 × 3.2	33.7
15	3.4 × 4.0 × 3.0	21.4	7.0 × 4.1 × 3.2	48.1
16	3.5 × 4.4 × 4.2	33.9	5.7 × 3.5 × 4.0	41.8
Mean		24.3		29.7

Volumes were calculated using the formula for the volume on an ellipsoid

* $p = 0.10$ (two-sided paired Student's t test)

Discussion

The technique effectiveness rate, evaluated on contrast-enhanced MR images taken 1 day after the procedure, was 93.8%, which is higher than that of US-monitored cryoablation for liver tumors [8, 9]. Considering that our study protocol restricted us to a single session for each tumor, the 93.8% technique effectiveness rate was sufficiently high. This high rate may be explained by the fact that MR images during the procedure visualized the cryoprobes and ablation zones clearly in all patients. This is consistent with the reports from Silverman et al. [4] and Dohi et al. [6] for metastatic liver tumors. The limitations of US-guided and monitored cryoablation for hepatic tumors lies in the ability to destroy all of a tumor confidently with reliance on ultrasound for ablative margins [10]. Seifert et al. [11] suggested that the lack of a method to adequately monitor the freezing process in the depth of an organ did not allow the precise and complete destruction of lesions with cryoablation. Our results suggest that MR monitoring is one way to improve the accuracy of cryoablation compared to US-monitoring cryoablation. On the other hand, the technique effectiveness of RFA is higher than 98% with one or two sessions [12]. However, nine of 65 HCC tumors showed viable tumor remnants on immediate CT scans after a single session of RFA [13]. Therefore the actual effectiveness of the technique was 86.1%. Thus, our result is comparable with a single session of RFA.

The temperature near the surface of the iceball is not sufficiently low to destroy tumor tissues [14, 15]. For the complete destruction of liver tumors, ablation with appropriate margins beyond the tumor border is necessary. In our study, local tumor progression occurred in 2 patients whose minimum ablative margin was less than 5 mm. In another patient who experienced local progression, the ablation margin was good enough. We assume that perfusion-mediated tissue heating may have led to incomplete ablation in this patient [16]. This type of tumor progression may be reduced in cryoablation by placing the cryoprobes as close as possible to the blood vessels [14].

The overall survival and local tumor progression-free rates were 80.0 and 81.2% at 3 years. These are the same as the reported results of resection of small HCC in patients with preserved liver function [17]. Three-year survival rates of RFA for small HCC ranged from 60 to 70% [8, 18]. Although our study was very small, our resulting 3-year survival rate is comparable or superior to RFA and the local tumor progression-free rate is comparable to a single session of percutaneous RFA (79.6%) [19]. Our results for overall survival and local tumor progression-free rates are encouraging for non-surgical treatment, as we have not used surgical resection even for new foci in the liver during the follow-up period. The high effectiveness rate of this technique at the initial cryoablation may have been positively influenced by the survival rate of patients, but the number of patients is obviously too small to state this conclusively.

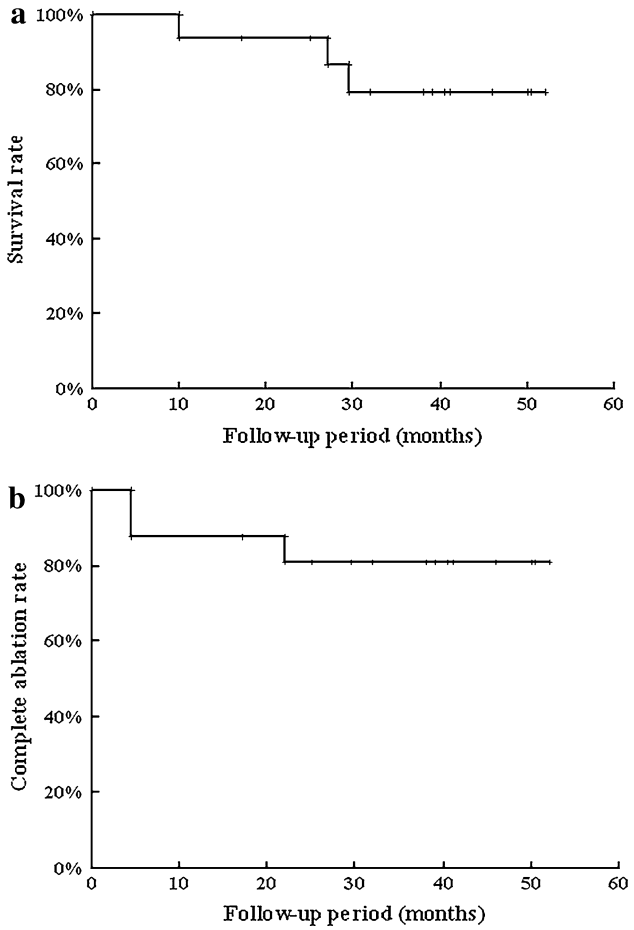

Fig. 3 Overall survival rate (**a**) and complete ablation rate (**b**) after single session of cryoablation

The immediate complications of the insertion technique were pneumothorax in one patient and hemothorax in another. We noticed that these complications occurred when we penetrated a cryoprobe at the costophrenic angle. The exercise of caution in this procedure, and/or improvements in equipment are necessary in order to reduce the occurrence of complications.

Sarantou et al. [20] have reported that cryoablation can produce adverse effects such as decreased platelet count, myoglobulinemia, parenchymal fracture, hypothermia, and cryoshock. In our study there were no serious immediate complications related to freezing and thawing, such as cryoshock, parenchymal fracture, or bleeding. Even when a tumor touched the capsule of the liver, we were able to complete the procedure without fracture of the hepatic parenchyma, bleeding, or injury to the adjacent organs. Periprocedural complications were mild disturbances of biochemistry, and most of these patients recovered spontaneously within 2 weeks. One patient experienced a rupture of the ablation zone 4 months after the procedure without serious consequences; this may have been lucky, since drainage was possible by the spontaneous fistula toward the skin surface. In general, morbidity from cryoablation is related to the volume of frozen tissue, the number of freeze-thaw cycles, and the number of cryoprobes [20]. Complication rates due to cryoablation ranged from 8 to 41% as the results of this study show. On the other hand, a multi-centered study of RFA for small HCC has reported rates of major and minor complications at 2.2 and $\leq$ 5%, respectively [21]. They were lower than our complication rate. There might be two possible reasons for the high complication rate in our study. First, this clinical trial was an initial experience for us and second, the diameters of the cryoprobes were larger than the diameters of RF needles. Recently, new cryoprobes with a small diameter (17G) have been developed. It is probable that the complication rate would be reduced using the new probe.

We measured the 24-hour ablation volume on gadolinium-enhanced dynamic MR images 1 day after the procedure. The 24-h ablation zone volume was at least 10% larger in 11 of the 16 patients. In another study, the 24-h ablation volume was reported to be larger in 5 of 18 metastatic liver tumors [4]. This phenomenon may relate to thrombosis of small vessels: among the three major mechanisms of tissue destruction under very low temperature, only vascular obstruction can have an effect outside of the iceball. The animal experiments showed the average size of the perfusion defect on Gd-enhanced MR image was larger than the iceball and correlated very well to the tissue necrosis on histopathologic examination [22, 23]. In clinical practice, we should be careful to prevent normal tissue complications because of the possibility of larger ablation beyond the iceball.

To date, RFA is the most popular minimally invasive thermal ablation modality. However, there are some advantages to cryoablation over RFA. First, cryoablation is pain free. We are able to treat patients without additional anesthesia especially for tumors located on the surface of the liver. Additionally, the local recurrence rate of subcapsular HCCs is higher than deeply located tumors during a single session of RFA [13]. Second, multiple probe placement makes a tailor-made shape of the ablation zone and the zone is clearly visible on MR images with multislice and multi-directional planes. Thus, we are able to place cryoprobes precisely into the tumor just beneath the diaphragm. We can also control the size and shape of the ice-ball to prevent cryo-injury of the adjacent organs.

In conclusion, MR-guided percutaneous cryoablation appears to be a feasible modality and potentially good option for the treatment of small HCC.

Acknowledgment This study is supported by HITACHI Medical Corporation.

References

1. Gage AA, Baust J. Mechanisms of tissue injury in cryosurgery. Cryobiology. 1998;37:171–86.
2. Onik G, Cooper C, Goldberg HI, Moss AA, Rubinsky B, Christianson M. Ultrasonic characteristics of frozen liver. Cryobiology. 1984;21:321–8.
3. Isoda H. Sequential MRI and CT in cryosurgery—an experimental study of rat. Nippon Igaku Hoshasen Gakkai Zasshi. 1989;49(12):1499–508.
4. Silverman SG, Tuncali K, Adams DF, et al. MR imaging-guided percutaneous cryotherapy of liver tumors: initial experience. Radiology. 2000;217(3):657–64.
5. Zhou X, Tang Z. Cryotherapy for primary liver cancer. Semin Surg Oncol. 1998;14:171–4.
6. Dohi M, Harada J, Mogami T, Fukuda K, Toyama Y, Kashiwagi H. MR-guided percutaneous cryotherapy of malignant liver tumor under horizontal-magnetic open system: initial experience. J Hepatobiliary Pancreat Surg. 2003;10(5):360–5.
7. National Cancer Institute. Cancer therapy evaluation program: common toxicity evaluation manual, version 2.0, 1999.
8. Jansen MC, van Hillegersberg R, Chamuleau RA, et al. Outcome of regional and local ablative therapies for hepatocellular carcinoma: a collective review. Eur J Surg Oncol. 2005;31(4):331–47.
9. Adam R, Hagopian EJ, Linhares M, et al. A comparison of percutaneous cryosurgery and percutaneous radiofrequency for unresectable hepatic malignancies. Arch Surg. 2002;137(12):1332–9.
10. Helling TS. Realistic expectations for cryoablation of liver tumors. J Hepatobiliary Pancreat Surg. 2000;7(5):510–5.
11. Seifert JK, Junquinger T, Morris DL. A collective review of the world literature on hepatic cryotherapy. J R Coll Surg Edinb. 1998;43(3):141–54.
12. Livraghi T, Meloni F, Di Stasi M, et al. Sustained complete response and complications rates after radiofrequency ablation of very early hepatocellular carcinoma in cirrhosis: is resection still the treatment of choice? Hepatology. 2008;47(1):82–9.
13. Komorizono Y, Oketani M, Sako K, et al. Risk factors for local recurrence of small hepatocellular carcinoma tumors after a single session, single application of percutaneous radiofrequency ablation. Cancer. 2003;97(5):1253–62.
14. Rewcastle JC, Sandison GA, Muldrew K, et al. A model for the time dependent three-dimensional thermal distribution within iceballs surrounding multiple cryoprobes. Med Phys. 2001; 28(6):1125–37.
15. Saliken JC, Cohen J, Miller R, et al. Laboratory evaluation of ice formation around a 3-mm accuprobe. Cryobiology. 1995;32 (3):285–95.
16. Onik G. Cryosurgery. Hematology. 1996;23:1–24.
17. Poon RT, Fan ST, Lo CM, Liu CL, Wong J. Long-term survival and pattern of recurrence after resection of small hepatocellular carcinoma in patients with preserved liver function. Ann Surg. 2002;235(3):373–82.
18. Zavaglia C, Corso R, Rampoldi A, et al. Is percutaneous radiofrequency thermal ablation of hepatocellular carcinoma a safe procedure? Eur J Gastroenterol Hepatol. 2008;20(3):196–201.
19. Hori T, Nagata K, Hasuike S, et al. Risk factors for the local recurrence of hepatocellular carcinoma after a single session of percutaneous radiofrequency ablation. J Gastroenterol. 2003; 38(10):977–81.
20. Sarantou T, Bilchik A, Ramming KP. Complications of hepatic cryosurgery. Semin Surg Oncol. 1998;14(2):156–62.
21. Livraghi T, Solbiati L, Meloni MF, et al. Treatment of focal liver tumors with percutaneous radio-frequency ablation: complications encountered in a multicenter study. Radiology. 2003;226 (2):441–51.
22. Klotz HP, Flury R, Shönenberger A, Debatin JF, Uhlschmid G, Largiadér F. Experimental cryosurgery of the liver under magnetic resonance guidance. Comput Aided Surg. 1997;2:340–5.
23. Tacke J, Adam G, Haage P, Sellhaus B, Großkortenhaus S, Günther RW. MR-guided percutaneous cryotherapy of the liver: in vivo evaluation with histologic correlation in an animal model. J Magn Reson. 2001;13:50–6.